HRTEM assessment of Wurtzite and Zinc-Blende phases in GaAs nanowires for optoelectronic devices

Sònia Conesa Boj

Directors of Master's Thesis: Dr. Francesca Peiró i Martínez and Dr. Jordi Arbiol i Cobos

EME/XaRMAE/IN2UB, Departament d'Electrònica, Universitat de Barcelona,

Martí i Franquès, 1, 08028 Barcelona; e- mail: sconesa@el.ub.es

Semiconductor nanowires have recently attracted a lot of interest as potential building blocks for future electronic and optoelectronic nanodevices. In this work structural and optical properties of semiconductor nanowires are studied by means of high resolution transmission electron microscopy (HRTEM) and photoluminescence (PL) analysis respectively. Several samples of GaAs nanowires grown under different As_4 pressures are studied, and the presence of different optoelectronic properties are discussed in relation to the crystalline structures and defects found.

04. Nanomagnetism, Nanoelectronics and Nanophotonics: nanowires, HRTEM, PL.

I. INTRODUCTION

Semiconductor nanowires are potential building blocks for the future electronic and optoelectronic nanodevices [1]. Nanowires of III – V materials are particularly promising for optoelectronic applications, due to the direct bandgap and high carrier mobility of these materials [2]. A direct bandgap means that the minimum energy of the conduction band lies directly above the maximum energy of the valence band in momentum space. In a direct bandgap semiconductor, electrons at the conduction band minimum can combine directly with holes at the valence band maximum, while conserving momentum. The energy of the recombination across the bandgap will be emitted in the form of a photon. This is radiative recombination, also called spontaneous emission. Such properties open up new possibilities for bandgap engineering [3,4].

From the point of view of fundamental research nanowires are interesting due to their small sizes and quasi one-dimensionality. In particular quantum effects in their physical properties are the subject of active research especially for combinations of III-V materials. The intrinsic conductivity and the concentrations of the intrinsic carriers in a semiconductor are controlled by the ratio $\left(E_g / k_B T\right)$ between the width of the prohibited band and the temperature. When this ratio is large, the concentration of the intrinsic carrier decreases and the conductivity will be also low.

We can determine the values of the prohibited bands by means of photoluminescence (PL) techniques. In the process of direct absorption, a photon is absorbed by the crystal creating an electron (e^-) and hole (h^+) pair. Posterior recombination of these e^-- h^+ pairs creates new photons with energies that allow us to characterize the energy band structure.

In the last decade, the use of gold as nucleation and growth seeds has been the most successful method for the nanowire synthesis process [5]. The main problem with this technique is that gold is a fast-diffusing metal which therefore harms their semiconducting properties. This problem has been solved by using different metals as catalysts or by avoiding the very same use of catalysts.

In recent works, catalyst-free growth has been achieved by molecular beam epitaxy (MBE) techniques [6,7,8,9]. This type of growth is linked to the existence of a patterned SiO_2 surface, whose role is to provide nucleation sites on the surface imperfections. Nanowires grown with one of these

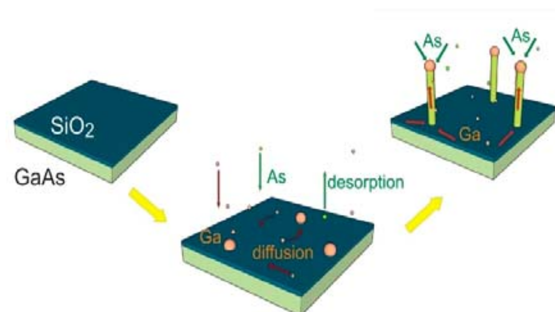

Fig. 1. Schematic representation of the Ga-assisted nanowire growth.

TABLE I

Sample	Pressure (mbar)	Ga growth rate (A/s)	NW growth rate (A/s)	Nomenclature
05-23-07.1	$3.5 \cdot 10^{-6}$	0.270	10.0	High beam flux (HBF)
06-27-07.2	$8 \cdot 10^{-7}$	0.251	4.0	Low beam flux (LBF)
06-23-07.3	$3.45 \cdot 10^{-7}$	0.251	0.9	Ultra low beam flux (ULBF)

TABLE I. Summary of the growth conditions for the different samples analyzed. Growth Temperature was 630ºC

techniques, Ga-assisted growth by MBE, are the subject of the present work.

Fig. 1 shows a schematic of the nanowires Ga-assisted growth. To start the growth, the mechanical shutters of the effusion cells for Ga and As are opened at the same time. Arsenic atoms impinging on the surface desorb immediately, due to the high substrate temperature. Ga atoms can chemisorb on the SiO_2 surface. This leads to the formation of Ga droplets, which subsequently act as a catalyst for nanowire growth. These droplets gather As atoms which are directly impinging the droplet. As the concentration of arsenic inside the droplet increases, a phase boundary in the binary phase diagram of the GaAs system will be reached and GaAs precipitates at the interface between the droplet and the substrate, leading to the growth of the nanowire. The growth of the nanowire is As limited, which means the growth rate is determinate by the flux of As. This dependence with the As is one of the main issues of this study.

On the other hand, is also crucial to fully understand the details of this growth mechanism, which are relevant to their optical and electronic properties [10,11]. An important tool towards this understanding is the nanowire structure characterization by means of high resolution transmission electron microscopy (HRTEM).

In the study of the different crystalline phases on the optoelectronic properties of the GaAs nanowires, we compare the PL measurements from single nanowires with the associated HRTEM analysis for the different growth conditions since each of these techniques provides complementary information on the nanowires behaviour and structure.

II. Experimental Setup

The GaAs nanowires were synthesized by MBE [8,9]. MBE is a technique for epitaxial growth via the interaction of one or several molecular or atomic beams that occurs on the surface of a heated crystalline substrate.

GaAs nanowires were grown in a high purity Gen – II MBE system. Two – inch [111]B GaAs wafers sputtered with a 10 – 20 nm thick silicon dioxide films were used as substrates. In order to ensure a contamination free surface, the substrates were dipped for 2s in a buffered HF (10% HF) aqueous solution (1HF:2H_2O), nitrogen blow dried, and transferred immediately after into the load lock of the growth chamber.

After the HF dip, the thickness of the remaining oxide was more than 6 nm in all cases. In order to desorb any remaining adsorbed molecules of the surface, the wafers were heated to 650ºC for 30 min prior to growth. The synthesis was carried out at a temperature of 630ºC. The arsenic (As_4) partial pressure was varied between high pressure and ultra low pressure, as can be seen in Table I. The Ga injection rate was varied from 0.12 to 0.82 Amstrong per second, and under rotation of 4 rpm.

As opposed to standard Vapour-Liquid-Solid (VLS) nanowires growth [12], no external metal catalyst like gold was used for the nucleation and growth of the nanowires. Instead as explained in [8,9], Ga droplets are formed in the SiO_2 surface which acts as natural catalyst for the nanowire growth.

The nanowires grow perpendicularly to the surface, following the [111]B direction. The interaction of the reactive gallium with the SiO_2 pinholes induces the formation of nanocraters, a key prerequisite for the nucleation of the nanowires [9,13]. The nanocraters reach the underlying substrate, resulting into a preferential growth orientation of the nanowires.

The morphology and structure of the nanowires with nanoscale resolution was characterized by means of High – Resolution Transmission Electron Microscopy (HRTEM) and Scanning Transmission Electron Microscopy (STEM) in a Jeol JEM2010F field emission gun microscope with a 0.19 nm point to point resolution.

For TEM sample preparation we mechanically removed the GaAs nanowires from the substrate and prepared a suspension in hexane. A drop of the previous suspension was then deposited on a holey carbon cupper grid.

Before introducing the sample into the microscope, it was introduced into the Plasma Cleaner for 15 minutes. The model of the plasma cleaner is a Fischione 1020. The Model 1020 Plasma Cleaner automatically and quickly removes organic contamination (hydrocarbon) from electron microscopy (EM) specimens and specimen holders. A low energy, reactive gas

plasma cleans without changing the specimen's elemental composition or structural characteristics.

For the optical characterization of the GaAs nanowires, micro photoluminescence (micro-PL) measurements were performed, by using a confocal attoCFM I setup from attocube system AG[a].

The Confocal attoCFM I is a standard tool for the investigation of optical properties of low dimensional structures. The GaAs nanowire samples are investigated at cryogenic temperature in order to reduce thermal noise and clearly observe quantization effects. In this system, the samples are maintained at a constant temperature below 10 K up to few days, after that a refilling with new liquid He is required. A recovery line is connected to the cryostat, in order to reliquify the consumed He gas.

Different lasers sources have been used in order to excite samples at different energy and thus study the PL spectra for the intensity of the radiated photons as a function of the photon energy. These are respectively a He-Ne laser (623 nm), a laser diode (780 nm) and two tunable lasers (in the range between 700 and 900 nm).

III. RESULTS

A. *Optical properties*

PL measurements were performed in order to analyse the optical properties of the nanowires grown at different pressures. For PL sample preparation we mechanically removed the GaAs nanowires from the substrate and transferred them to a piece of a Si wafer. Growth conditions are shown in table I.

Fig. 2a shows a spectrally and spatially resolved PL scan along the axis of the nanowire grown at High Arsenic Beam Flux. The orientation of the nanowires for the PL scan is such that the upper part of Figs. 2a, 2b and 2c corresponds to the seeds which originate the growth. As it can be seen, the PL emission spectrum turns out to be homogeneous along the entire length of the nanowire. The dependence of the PL spectra as a function of the excitation power is shown in Fig. 3a. The most relevant feature is a sharp peak at 1.515 eV. This peak corresponds to the decay of the free exciton as measured in bulk GaAs. In the energy region between 1.485 and 1.505 eV a broader peak can be observed Fig. 3a however its intensity is much lower than that of the main peak.

Fig. 2b shows the same PL scan as in Fig. 2a but now corresponding to the Low Arsenic Beam Flux growth conditions. It can be observed that the spectrum is rather different than its HBF counterpart. The spectrally resolved scan along the axis of the nanowire shows different spots of emission in the region between 1.45 and 1.51 eV. The power series taken at fixed position Fig. 3b shows several sharp peaks.

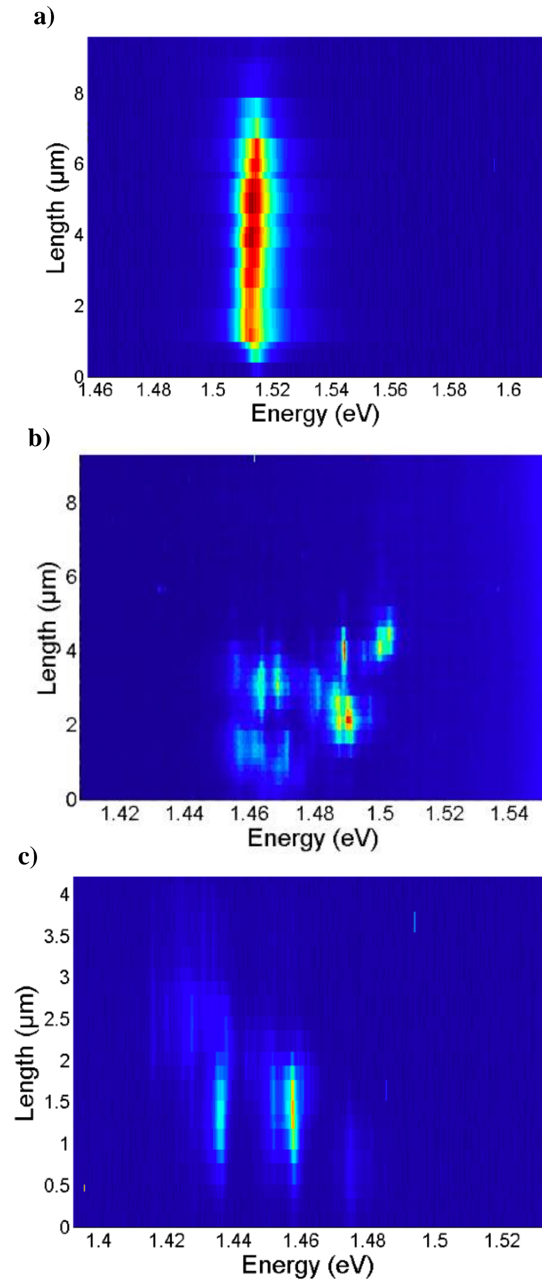

Fig. 2: (a), (b) and (c) energetically resolved photoluminescence scan along the axis of the nanowires grown under HBF, LBF and ULBF conditions respectively.

In the case of ULBF Fig. 2c shows the analogue PL results. In this case the nanowires were grown at the lowest pressure of arsenic possible. We observed several peaks with the lowest transition energy at 1.425 eV, and with the most intense emission found near 1.46 eV. No emission at 1.515 eV was observed as opposed to the previous cases. Fig. 3c show a power series obtained on ULBF nanowire. We can see several peaks placed below 1.47 eV.

[a] www.attocube.com

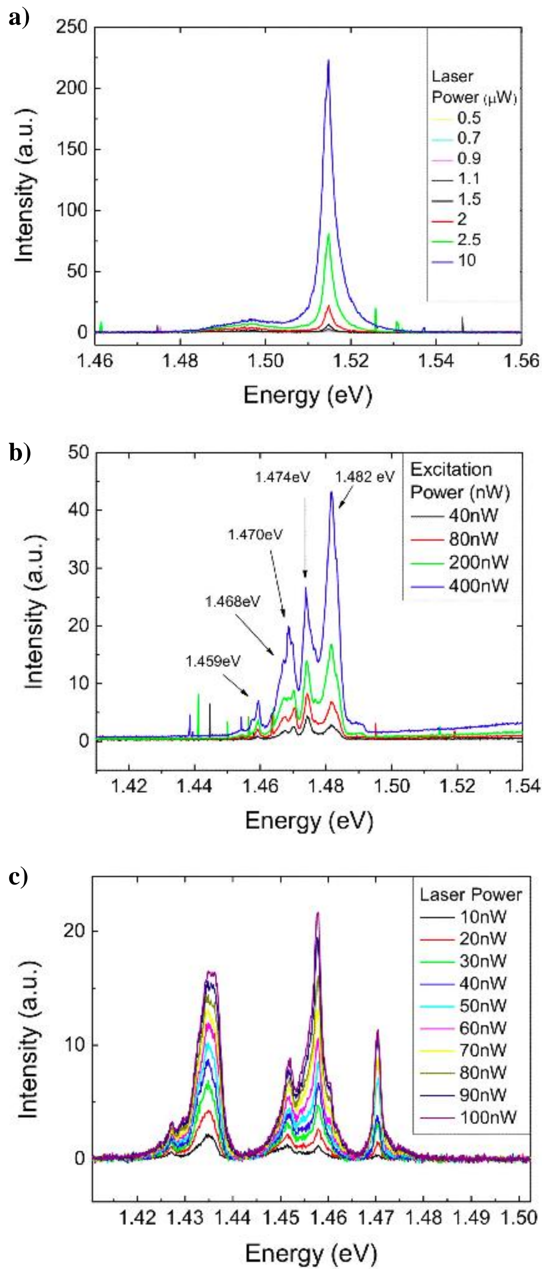

Fig. 3: (a), (b) and (c) PL spectra of the HBF, LBF and ULBF nanowires under different excitation powers respectively.

One possibility to explain the anomalous transitions in PL spectra could be the presence of impurities, homogeneously distributed along the nanowire. Alternatively, changes in the nanowire structure or presence of crystal defects would yield to a similar signal [14]. Nevertheless this point will have to be analyzed in more detail in the following section.

In order to further understand the origin of the different behaviours observed in the PL spectra as function of the growth conditions (As flux), we will perform a detailed HRTEM analysis for each of the available samples.

B. Crystalline structure

Transmission Electron Microscopy (TEM) is a technique which allows obtaining structural information of materials at the nanoscale.

The instrument can be used to produce electron-diffraction patterns (SAED), useful for analyzing the properties of a crystalline specimen. In this technique an aperture can be inserted in the image plane of the objective lens, to limit the area of the specimen which contributes to the diffraction pattern.

By selecting the object of the intermediate lens to be the image plane of the objective lens, we can project an image of the sample onto the screen. It is also possible to distinguish two basics imaging modes, bright-field (BF) and dark-field (DF) imaging.

By selection of the bright spot in the middle of the SAED pattern, this corresponds to the direct beam of unscattered electrons; a BF image of the sample is formed. By selection of other spots of the SAED pattern only scattered electrons contribute to the image, which is called a DF image.

High resolution transmission electron microscopy (HRTEM) is another imaging mode of the TEM. This mode allows the image of the crystal structure of a sample at atomic scale.

In Fig. 4 we show the standard process which we have followed in order to analyze our specimens. First of all, we obtain low resolution bright-field (BF) TEM images in order to observe the sample morphology. A BFTEM micrograph of several GaAs nanowires grown under ULBF conditions is shown in Fig. 4a. Dark and bright alternative contrast stripes along the growth axis are observed. The Ga-rich catalyst droplet responsible for the Ga-assisted growth can be seen at the left end of the nanowire. The other extreme of the nanowire shows the last stages of the nanowire growth, those parts nearer to the sample substrate.

After analyzing the sample morphology, a deeper analysis at atomic scale is needed. In this way, we select a GaAs nanowire and tilt it in order to find a low index zone axis. Once we have done it we proceed in order to obtain the HRTEM micrographs (Fig. 4b).

From HRTEM images we obtain the fast Fourier transform (FFT) or Power Spectrum, which can be indexed and thus used to obtain the crystallographic information of the sample (Fig 4d-f). In the example shown in Fig.4, HRTEM measurements realized on the GaAs NW determined that the growth direction was [1-11] being the observation zone axis the [110]. Each color of the Power Spectra in Figs. 4d-f, correspond to different crystalline structures present in the

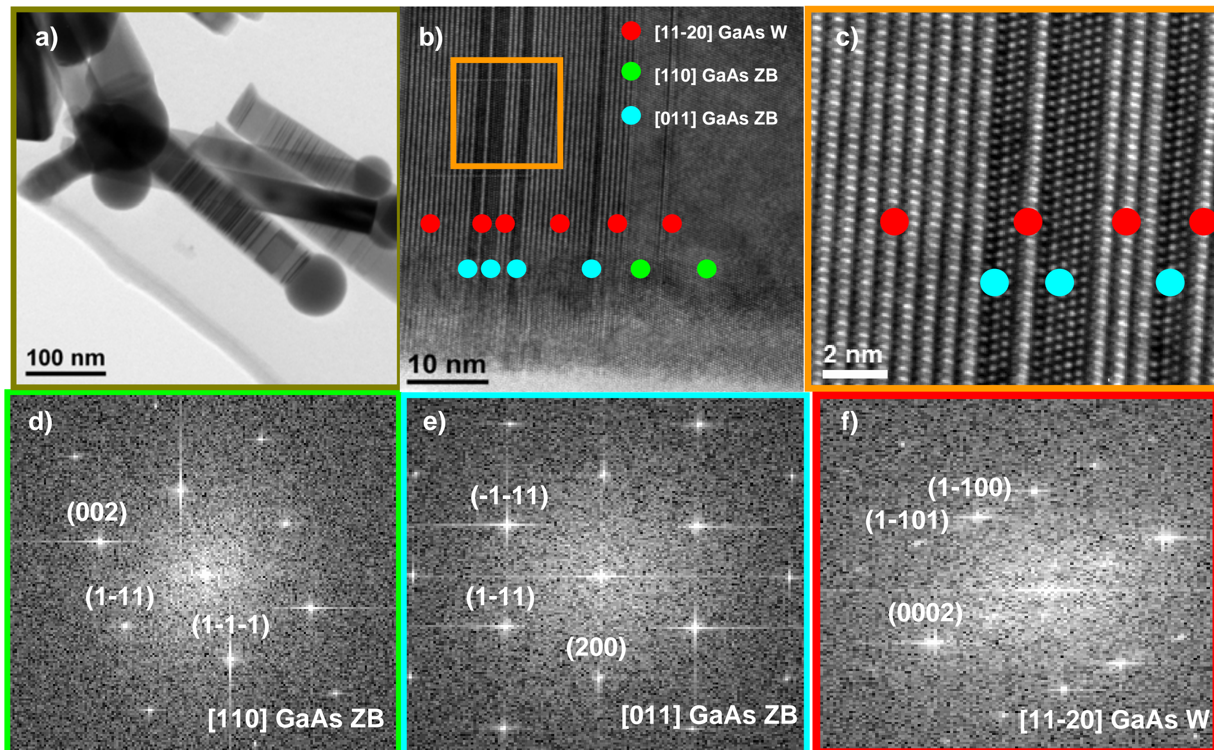

Fig. 4: (a) BF image of a GaAs nanowire grown under ULBF conditions; (b) and (c) HRTEM image of one region of the nanowire; (d)-(f) Power spectra that correspond to different crystalline structures present in the nanowire.

nanowire. These spectra can be attributed to the GaAs wurtzite (WZ) crystal structure (red) and the GaAs Zinc-Blende (ZB) crystal structure in [110] and [011] orientations, green and blue, respectively.

The sections of ZB marked blue and green differ in the relative orientation of the crystal to the electron beam. The dot of green colour is placed on a (110) surface while the blue colour dot on a (011).

Normally the formation of the W phase can be related to the amount of Ga As in the gold droplet. In our case Ga adopts the role of the catalyst droplet. Hence, the supersaturation and the growth rate depend on the arsenic pressure.

In order to investigate the dependence of the nanowire crystalline structure as a function of the growth conditions, we studied three GaAs nanowire samples for three different Arsenic partial pressures. The cases are High Beam Flux, Low Beam Flux and Ultra Low Beam Flux, see Table I.

B.1. High Beam Flux

The BFTEM image shown in Fig. 6a is a representative of the nanowires grown under HBF conditions. These nanowires are in general long in the axial direction and narrow in the radial direction. The average length of these nanowires is 6μm. On the other hand, the average width of these nanowires turns out to be 48 nm. Both lengths have been determined from the TEM measurements using the Digital Micrograph software.

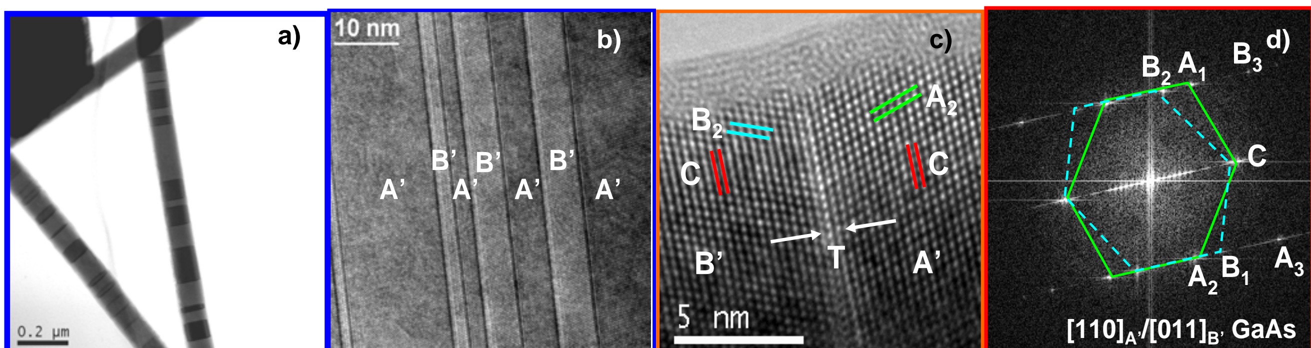

Fig.6: (a) BF- images correspond to NWs grown under HBF conditions; (b) Region of multitwinned; (c) HRTEM image and (d) the power spectrum of the HRTEM image.

TABLE II

A' Spot #	Indexation	B' Spot #	Indexation
A_1	(002)	B_1	(200)
A_2	(1-1-1)	B_2	(-1-11)
A_3	(2-20)	B_3	(0-22)
Zone Axis: [110] GaAs		Zone Axis: [011] GaAs	

TABLE II. Indexation of the spots corresponding to the A' and B' in Fig. 6d.

In Fig. 6b we can observe stripes of different contrast along the growth direction of the nanowire, labeled by A' and B'. These striping of different contrasts correspond to twin segments. We observe a high density of twins along the [1-11] growth direction. The structural analysis of one of these twin boundaries is shown in Figs. 6c-d.

Fig. 6d corresponds to the power spectra of Fig. 6c and represents a twin boundary of the nanowire. This reflects the difference between the two orientations, the pattern diffraction corresponding to the crystalline structure of ZB. These regions are related by a 60º rotation of the crystal along the [1-11] growth axis. As described before, we will assign the colors green and blue to each of two orientations [110] and [011] of the ZB respectively. In the table II we show the correspondence between the plot labels and the indexation of the two power spectra which appear in Fig. 6d.

The percentage of the appearance of both ZB orientations is of 49% and 49% of the total nanowire amount, respectively. The power spectrum analysis around a small region of the nanowire located at the lower end, corresponding to the beginning of the growth, shows the presence of the W phase. The total amount of W is approximately a 2%.

In summary, the nanowires grown under HBF conditions showed pure ZB structure along almost their length, with twins along the axis of the nanowire. Twinning occurs nonperiodically along the nanowires. In the nanowire grown under HBF conditions, there is a long segment of ZB GaAs rich structure.

B.2 Low Beam Flux

The TEM image shown Fig. 7a correspond to a nanowire grown under LBF conditions (intermediate As_4 pressure). Growth is slower than in the case of high As_4 content, thus nanowires are shorter with lengths ranging from 1200 to 1500 nm. Under these conditions the average width is 50 nm, slightly larger than under HBF.

In all the studied nanowires there are three characteristic regions. The first region Fig. 7b corresponding to the last growth stage and placed just below the Ga catalytic seed. This region has a width ranging from 20 to 40 nm. As we can observe, this region has a large density of very narrow stripes of different contrasts. This region can be described as a multitwinned area, and might have presence of thin W segments.

The second region Fig. 7c is the most extended area and comprises the middle part of the nanowire. It is ranging from 800 to 1100 nm and is composed of longer stripes of different contrast wide segments up to 800 nm. This area is

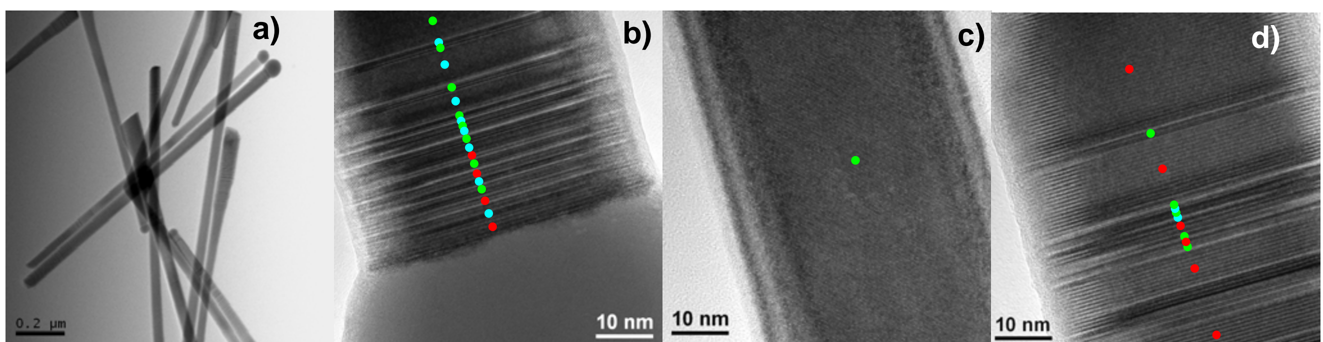

Fig. 7: (a) correspond to nanowires grown under LBF conditions. There are three characteristic regions: (b) it is a multitwinned ZB area which may have thin W segments, (c) and is composed of pure ZB wide segments and (d) in this area there is a mixture of W and ZB segments.

characterized for having low presence of twin defects from 3 to 5 along the whole region and is composed of pure ZB.

The third region Fig. 7d corresponds to the one nearer to the substrate, and it is characterized for having a high density of twin defects and also a wide presence of W phase.

The segments of W are longer than the ones obtained under HBF conditions and can be as large as 35 nm. Compared to the case of HBF nanowires, the part of the nanowire in which W is found is somewhat shorter. This region containing W is found to extend from 150-400 nm that is 10-30% of the total length of the nanowire.

The Ga droplet which catalyzed the growth can be seen at one end of the nanowire in Fig. 7b. The power spectrum analysis shows that these nanowires have long segments of the W crystal structure which is formed during the initial phases of growth since it is located near these Ga droplets, and is separated by thin ZB layers.

B.3 Ultra Low Beam Flux

The bright field BF image shown in Fig. 4a is a representative of the nanowire grown under ULBF conditions. In general, these nanowires are shorter than the nanowires grown at the higher pressure. The average length of these nanowires is the 350-400 nm. In this case, the typical widths of the nanowires range from 50 up to 55 nm. The nanowires grown under these conditions have the longest W segments which were obtained among the various samples, with lengths up to 65 nm. The remaining regions of the nanowire show the ZB crystal structure with decreasing density of twin boundaries.

In the following section, the correspondence of each region with the different crystalline structures and their correlation to the PL results will be discussed in more detail.

IV. Discussion

At ambient pressure, many of the III–V binary semiconductors adopt in general the cubic zinc blende (ZB) structure, which has ideal tetrahedral coordination [15]. However, GaAs may adopt under certain conditions the closely related hexagonal Wurtzite (W) structure. Within the same NW the two structures may coexist (phenomenon known as ZB – W polytypism), and their relative abundance depends for example on the pressure conditions under the growth process. The alternation of W and ZB crystalline structures has been observed recently in different materials when grown as nanowires even under low pressure conditions. In the case of GaAs several works have been published in the last few years dealing on this topic [16,17,18].

The hexagonal wurtzite (W) structure is also fourfold coordinated but with an *ababab*… stacking sequence along the hexagonal [0001] axis rather than the *abcabc*… stacking of zinc blende along its cubic [111] axis (see Fig. 8). The

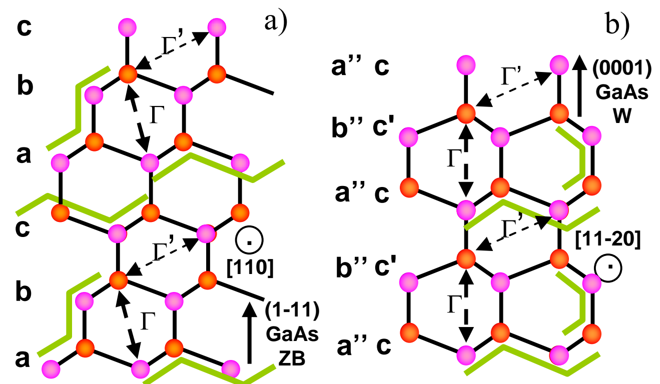

Fig. 8: (a) Atomic scheme of the GaAs Zinc-Blende (ZB) structure with the regular *abcabc* stacking of close-packed layers; (b) Atomic scheme of the GaAs Wurtzite (W) structure with the *a¨b¨a¨b¨a¨ or equally c/c'/c/c'/c* arrangement of the <0001> planes.

close similarity of these two structures, which differ only in the geometry of bonding of their third – nearest neighbours, results in only small differences in their internal energies, leading to ZB-W polytypism in GaAs [19].

Also in the case of Si nanowires a similar phenomenon has been reported, too [20,21]. In the case of Si nanowires, the synthesis of wurtzite nanowires has been demonstrated for the first time in [20], using standard CVD on oxidized Si substrates. It has been shown that the synthesis of silicon nanowires with Cu as a catalyst via the vapour-solid-solid process presents changes continuously along the growth direction from diamond (zinc-blende in the case of binary compounds) to wurtzite (both being semiconductor Si phases) [21]. The coexistence of phases within a Si nanowire is a new phenomenon intrinsic to the use of Cu as a catalyst.

Just at the beginning of the nanowire grown under ULBF conditions, we can find twins in the appearance of twins along the growth axis in III-V and group IV nanowires is a common phenomenon and has been observed by others authors [22,23,24].

HRTEM measurements were realized to analyse in detail the structure of the nanowires. The power spectrum of the HRTEM images was calculated and the angles and distances between the planes obtained with the program Digital Micrograph. The structure of the nanowires was studied as a function of the growth conditions summarized in table I.

The PL spectra observed in Figs. 3b and 3c could be understood as a manifestation of the type of band alignment of the heterostructures formed by alternating WZ and ZB sections, with the associated formation of quantum wells, as we will discuss in more detail below.

The band gap of W GaAs is higher than that of ZB GaAs by 33 meV and that a W-ZB GaAs heterojunction has staggered band alignment with the W conduction band 117meV above

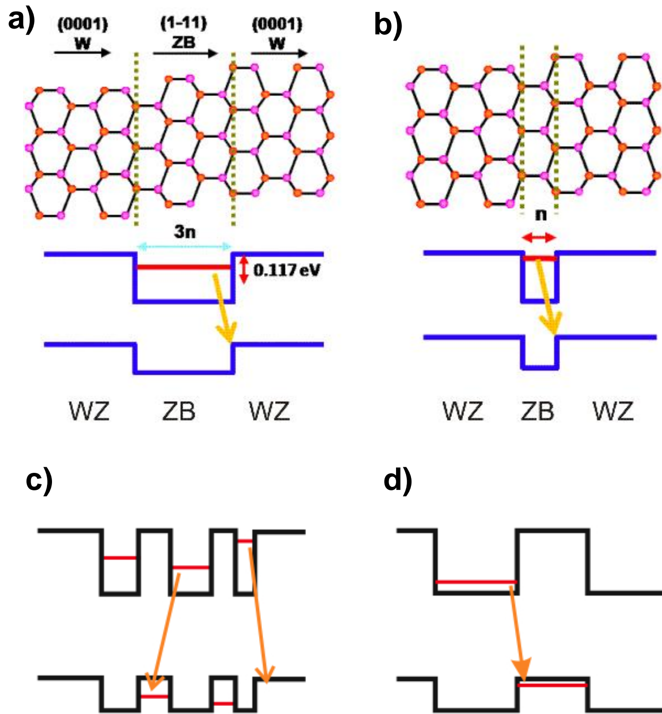

Fig.9: The upper figures (9a and 9b) show the sketch of the formation of QW leading to the confinement of the electrons for two different widths of the heterostructures. The lower figures (9c and 9d) show that the width of the QW dictates the effects of the heterostructures in the energy of the observed electronic transitions.

the ZB conduction band, and the W valence band 84meV above that of ZB Fig. 10.

Twinned nanowires can be regarded as a series of ZB wells with varying widths separated by thin W barriers. Photoexcited electrons and holes are spatially separated in the heterojunction. This space charge induces an electric field and band bending, which modifies the electron and hole energy levels via the Stark effect, thus leading to the PL peaks shift.

A similar effect has been previously reported in quantum wells with staggered band alignment [25]. We believe that the PL spectra observed in Fig.3 are a manifestation of the type of band alignment of the heterostructures formed by alternating WZ and ZB sections.

In order to better correlate the PL measurements with the information on the nanowires structure obtained by HRTEM qualitative estimations can be performed considering the basic characteristics of the crystalline structures of the nanowire. It is important to take into account the situation in which one segment of ZB or W crystal structure is embedded in the other type as is the case in our nanowires.

This situation is known as a Quantum Well (QW) since due to the band offsets at the interfaces one type of carrier will be confined to a potential well, as we can see schematically in Figs. 9a and 9b. Fig. 9a shows this situation for a thick W-ZB-W QW, while Fig 9b shows the same situation for a slightly thinner W-ZB-W QW, which leads to bigger confinement energy.

Without entering into details the situation can be thought as the analogue of the particle confined in a one dimensional potential but with the quasiparticle formalism relevant for bulk crystalline materials. The net effect of the formation of these QWs is the modification of the bandgap, and thus of the energy of the transitions which have been observed in PL due to this confinement energy, dictated by the thickness of the QW.

Now we discussed how these considerations for the bands structure of GaAs nanowires can help in the interpretation of the results presented in the previous section.

For nanowires grown under HBF conditions we observed homogenous emission along the axis, and TEM showed that they were composed almost 98% by ZB. For these reasons, it is natural to think that the 1.515 eV PL peak comes from the ZB region of the nanowire since this value reproduces the known energy of the free exciton in bulk GaAs (ZB).

On the other hand TEM analysis also shows thin segments of W near the end of the nanowire with dense spacing of ZB twins. In this case it is expected the formation of W-ZB-W narrow QW with rather large confinement energies, which imply the transitions observed in the spectral region from 1.49-1.5 eV, this situation is illustrated in Fig. 9c.

For the nanowires grown under LBF conditions PL analysis showed localized states while TEM analysis determined a mixture of W and ZB phases, up to a length of 30% of the nanowire where the W segments were typically longer than in the previous case. This implies that the QWs which are formed should have larger widths and therefore less confinement energies for holes and lower transition energies as indeed it is observed in Fig. 9d.

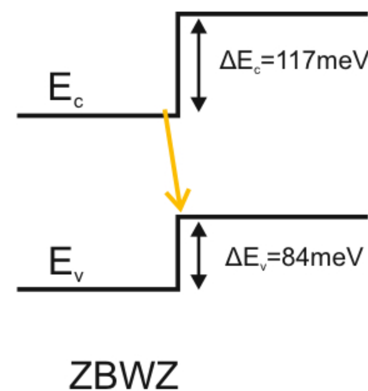

Fig. 10 W-ZB GaAs heterojunction has staggered band alignment with the W conduction band 117meV above the ZB conduction band, and the W valence band 84meV above that of ZB.

Finally for the nanowires grown at ULBF conditions PL emission was observed down to 1.425 eV and strong emission was measured located around 1.46 eV. On the other hand TEM measurements determined that under this conditions the grown nanowires had very long pure W sections with extensions up to 65 nm.

The strong emission could be related to the formation of a nonperiodic superlattice, while the lowest transition energy should be attributed to a transition between long sections of the nanowire with W and ZB crystal structures respectively.

V. CONCLUSION

The goal of this thesis of master was to understand the anomalous PL spectra observed in catalyst-free GaAs NWs when grown under different As pressure conditions. TEM analysis at atomic scale showed that the defects and crystal structure changes in GaAs could be responsible of the differences observed in their optoelectronic properties. It was shown that the appearance of twin defects in ZB and also the appearance of W phase domains along the NW growth axis is the responsible of the red shifted peaks in PL spectra.

We can summarise the optical properties of W and ZB based heterostructures. First of all, the PL peaks observed range from 1.42 to 1.52 eV approximately, where the upper value corresponds to the decay of the free exciton in bulk GaAs. The peaks between 1.48-1.50 eV correspond to the ZB QW which appears in W during the initial phase of the nanowire growth.

On the other hand, the peaks measured in the vicinity of 1.41 eV are originated from the opposite situation, namely the formation of W QW in ZB. And other important region is the range between 1.46 eV -1.48 eV which comes from a superlattice of ultra thin ZB and W QWs. Finally the lower limit in the spectrum originates from recombination at the W-ZB interface.

In conclusion, our study shows that there is large room for improvements on the control of the optoelectronic properties of semiconductor nanowires. Such properties can be modified to suit our needs by tuning the nanowire crystalline structure with suitable modifications of their growth conditions. This study is therefore relevant due to the large recent interest in bandgap engineering for the new generation of nano-optoelectronic devices.

ACKNOWLEDGEMENTS

I would like to thank Dr. A. Foncuberta i Morral, D. Spirkoska, M. Heigoldt and C. Colombo from Walter Schottky Institute (Garching Germany) for sample preparation and PL measurements. I would also like to thank the Serveis Cientificotècnics of Universitat de Barcelona to let me use their microscopy facilities. I'm especially grateful to the directors of this Master Thesis, Dr. Francesca Peiró and Dr. Jordi Arbiol for their continued encouragement and assistance and for giving me the opportunity of participate in this interesting research project.

REFERENCES

[1]Li, Y.,; Qian, F.; Xiang, J.; Liebre, C. M. Mater. Today , 9, 18-27 (2006)
[2] H. Petterson, L. Samuelson, et al Nano Lett, 6, 229-232 (2006)
[3] Huang, Y.; Lieber, C. M. Pure Appl. Chem., 76, 2051 (2004)
[4] Samuelson, L.; et al Physica E, 25, 313 (2004)
[5] Yong Kim, Hannah J. Joyce, Qiang Gao, H. Hoe Tan, et al, Nano Lett. 6, 599-604 (2006)
[6] J. Arbiol , S. Conesa-Boj, J. Rebled, F. Peiró, A. Foncuberta i Morral, D. Spirkoska, , M. Heigoldt, J. R. Morante, and G. Abstreiter, to be published (2008)
[7] Florian Furtmayr, Martin Vielemeyer, Martin Stutzmann, Jordi Arbiol, Sònia Estradé, Francesca Peiró, Joan Ramon Morante, Martin Eickhoff. Journal of Applied Physics, 104 (3), 034309 (2008)
[8] C. Colombo, D. Spirkoska, M. Frimmer, G. Abstreiter, and A. Fontcuberta i Morral, Phys. Rev. B 77, 155326 (2008)
[9] A.F.I. Morral, C. Colombo, G. Abstreiter, J. Arbiol, J.R. Morante, Applied Physics Letters, 92, 063112 (2008).
[10] P. Nguyen, H. T. Ng, T. Yamanda, M. K. Smith, J. Li, J. Han, and M. Meyyappan, Nano Lett. 4, 651 (2004)
[11] J. B. Gonzalez-Diaz, A. Garcia-Martin, G. Armellas, D. Navas, M. Vazquez, K. Nielsch, R. B. Wehrpohn, and U. Gosele, Adv. Mater. 19, 2643 (2007)
[12] R. S. Wagner and W. C. Ellis, Appl. Phys. Lett. 4, 89 (1964)
[13]A.F.I. Morral, K. Maslov, C. Colombo, G. Abstreiter, J. Arbiol, J.R. Morante, Applied Physics Letters, 92, 149903 (2008).
[14]J. Bao, D. C. Bell, F. Capasso, J. B. Wagner, T. Martensson, J. Trägardh and L. Samuelson Nano Lett 8, 3, 836-841 (2008)
[15] A. Mujica, A. Rubio, A. Munoz, and R. J. Needs, Rev. Mod. Phys. 75, 863 (2003)
[16] Ihn S G, Song J I, Kim T W, Leem D S, Lee T, Lee S G, Koh E K and Song K , Nano Lett. 7, 39 (2007)
[17] Ihn S G, Song J I, Kim Y H and Lee J Y, Appl. Phys. Lett. 89 053106 (2006)
[18] A. Foncuberta i Morral, J. Arbiol, S. Conesa-Boj, S. Estradé, F. Peiró, J.R. Morante et al., to be published.
[19] C.-Y. Yeh, Z. W. Lu, S. Froyen, and A. Zunger, Phys. Rev. B 46, 10086 (1992)
[20] A Foncuberta I Morral, J Arbiol, D. Prades, A Cirera and J R Morante Adv. Mater 19, 1347-1351 (2007)
[21] J.Arbiol, B Kalache, Pere Roca i Cabarroca, J R Morante and A Foncuberta i Morral Nanotechnology , 18, 305606 (2007)
[22] Korgel, B. A. Nat Mater 5 (7), 521-522 July (2006)
[23] J. Arbiol, S. Estradé, F. Peiró, B. Kalache, P. Roca i Cabarrocas, J. R. Morante, A. Foncuberta i Morral, J. Appl. Phys. in press (2008)
[24] J Arbiol, B Kalache, Pere Roca i Cabarroca, J R Morante and A Foncuberta i Morral Nanotechnology, 18, 305606 (2007)
[25] Fouquet, J E; Minsky, M S; Rosner, S J, Appl. Phys. Lett, 63, 3212-3214 (1993)